Materials Plus
https://ojs.wiserpub.com/index.php/MP/

Research Article

Modeling of Cr^{3+} doped Single Crystals of Lithium Sulfate Monohydrate

Maroj Bharati[1], Vikram Singh[1], Ram Kripal[2*]

[1]Department of Physics, Nehru Gram Bharti (DU), Jamunipur, Prayagraj, India
[2]EPR Laboratory, Department of Physics, University of Allahabad, Prayagraj-211002, India
E-mail: ram_kripal2001@rediffmail.com

Received: 4 April 2024; **Revised:** 25 April 2024; **Accepted:** 28 April 2024

Abstract: Crystal field parameters and zero field splitting parameters of Cr^{3+} doped lithium sulphate monohydrate, $Li_2SO_4.H_2O$ single crystals are computed with the help of superposition model. The appropriate sites for Cr^{3+} ions in $Li_2SO_4.H_2O$ with distortion are considered for calculation. Theoretical zero field splitting parameters obtained including local distortion in the calculation correspond well with the values obtained from the experiment. The optical energy bands for Cr^{3+} in $Li_2SO_4.H_2O$are evaluated with the Crystal Field Analysis Program and crystal field parameters. The results suggest that Cr^{3+} ions substitute for one of the Li^+ ions, and the charge compensation occurs by the proton vacancies in $Li_2SO_4.H_2O$ single crystals.

***Keywords*:** superposition model; crystal field; zero-field splitting; optical spectroscopy; Cr^{3+} ions in $Li_2SO_4.H_2O$

1. Introduction

The electron paramagnetic resonance (EPR) provides the nature of the electric field symmetry produced by the ligands about the paramagnetic ions, permits the determination of the flaw causing the charge compensation in impurity doped crystals [1] and the zero field splitting (ZFS) of impurity ions added to crystals [2-4]. Superposition model (SPM) [5-7] is used most commonly for theoretically determining zero field splitting (ZFS) and crystal field (CF) parameters.

Lithium sulphate monohydrate single crystals have a wide spectrum of applications in non-linear optical (NLO) assistant devices used in telecommunications, laser technology, THz imaging, optical communication, and optical storage technologies [8]. The optical, electrical, and thermal properties of this crystal mark it as a potential candidate for modern optoelectronic applications [9]. It is found that the intoxication of a dopant in lithium sulphate monohydrate increases the efficacy of the grown single crystals [8].

Cr^{3+} ions have extensively been used as probe to study the symmetries of the crystalline electric fields. An important interest is the compensation of the charge imbalance when divalent or trivalent impurities are incorporated in place of monovalent ions. In these cases positive ion vacancies are supposed to fulfil the charge compensation [10]. Incorporated impurities yielding microscopic structural change affect the optical properties of the crystal. The Cr^{3+} ion is a very good probe for obtaining information on lithium sulphate monohydrate, $Li_2SO_4.H_2O$ crystal [11].

EPR measurements for Cr^{3+} ions in $Li_2SO_4.H_2O$ were done and spin Hamiltonian parameters reported [11]. The consistency of the EPR spectra with the monoclinic symmetry of the crystal indicates the substitution of Cr^{3+} at Li^+ site. The ionic radius of Li^+ ion (0.078 nm) is larger than that of the Cr^{3+} ion (0.0615 nm). Therefore

DOI: https://doi.org/10.37256/3120244696

Cr^{3+}substitutes for one of the Li^{+} ions, and the charge compensation takes place in this case by the proton vacancies, since no superhyperfine of the protons with the electron spin of Cr^{3+} was observed [11].

The laboratory axes (*x*, *y*, *z*) are selected so that they align with the crystallographic axes (*a**, *b*, *c*). The symmetry adopted axes (magnetic axes) are labeled (*X*, *Y*, *Z*). The principal *Y* axis of **g** and **D** tensors of Cr^{3+} ions is found corresponding to the crystallographic *c* axis.

This study examines the superposition model (SPM) of the CF parameters and the ZFS parameters for Cr^{3+} ions in $Li_2SO_4.H_2O$ crystal. Due to continued interest in the compound by other workers [12, 13], this study is undertaken. The objective is to find the ZFS parameters, the lattice distortion and the CF parameters for the Cr^{3+} ions in $Li_2SO_4.H_2O$ at octahedral sites. The optical energy bands for Cr^{3+} ions in $Li_2SO_4.H_2O$ are determined using CF parameters and Crystal Field Analysis (CFA) computer program. Both the ZFS and CF parameters obtained may be useful in future investigations for scientific and industrial applications of such crystals.

2. Crystal structure

$Li_2SO_4.H_2O$ crystallizes in a monoclinic crystal system with space group $P2_1$ [14]. The unit cell dimensions are a = 0.5454 nm, b = 0.4857 nm, c = 0.8173 nm, and β = 107.22°. The compound contains the two Li atoms Li_1 and Li_2, Li_1 being coordinated only to the oxygen atoms of the SO_4 groups, while one of the O atoms around Li_2 is the oxygen of the water molecule.$Li_2SO_4.H_2O$ crystal structure with symmetry adopted axis system (SAAS) is shown in Fig.1.

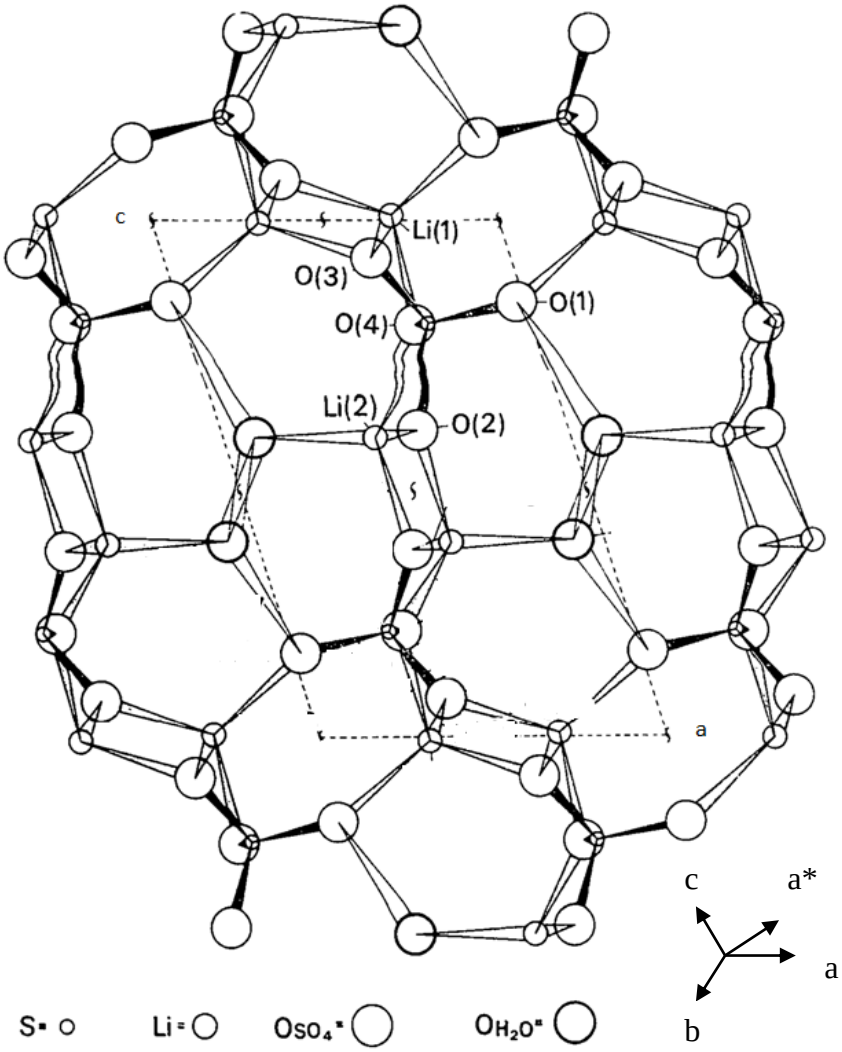

Figure 1. $Li_2SO_4.H_2O$ crystal structure with symmetry adopted axis system (SAAS)

The symmetry adopted axes (SAA) (local site symmetry axes) are the mutually perpendicular directions of metal-ligand bonds. The Z axis of SAAS is along the metal-ligand bond Li-O (crystal **a***-axis) and the two other axes (X, Y) are perpendicular to the Z axis for center I (Fig. 1). This indicates that Cr^{3+} substitutes for Li^+ in the crystal of $Li_2SO_4.H_2O$ with approximately orthorhombic symmetry and charge compensation. Cr^{3+} ion's ionic radius (0.0615 nm) is marginally smaller than Li^+ ionic radius (0.076 nm), indicating that Cr^{3+} ion can sit at the position of Li^+ with charge compensation and certain distortion.

Table 1 displays the ligands' spherical polar coordinates and Cr^{3+} ion position for center I in $Li_2SO_4.H_2O$ [14]. Cr^{3+} ion ZFS and CF calculations in $Li_2SO_4.H_2O$ use these data.

3. Calculations of zero field splitting parameters

The energy states of Cr^{3+} ions in crystals were obtained utilizing the spin Hamiltonian [15, 16, 17]:

$$\mathcal{H} = \mathcal{H}_{Ze} + \mathcal{H}_{ZFS} = \mu_B B.g.S + \sum B_k^q O_k^q = \mu_B B.g.S + \sum f_k b_k^q O_k^q , \quad (1)$$

where g, μ_B and $\boldsymbol{B}$ are the spectroscopic splitting factor, Bohr magneton and steady magnetic field, respectively. S represents the effective spin operator and $O_k^q(S_x, S_y, S_z)$ are the extended Stevens operators (ESO) [18, 19]; B_k^q and b_k^q give the ZFS parameters, f_k = 1/3 and 1/60 the scaling factors for k = 2 and 4, respectively. For the Cr^{3+} ion (S = 3/2) at orthorhombic symmetry sites, the ZFS terms in (1) are given as [20, 21]:

Table 1. The spherical polar co-ordinates (R, θ, ϕ) of ligands and fractional coordinates of Cr^{3+} ion (center I) in $Li_2SO_4.H_2O$ single crystal

Position of Cr^{3+}	Ligands	Spherical polar co-ordinates of ligands		
		R^A	θ^0	ϕ^0
ND: Substitutional	O1	6.7696	174.44	53.14
(0.3053, 0.4949, 0.9938)	O2	11.5987	165.26	-69.05
	O3	7.8598	162.05	-73.88
	O4	6.5226	169.07	82.38
	O1’	3.8625	133. 34	56.98
	O2’	4.8637	101.15	36.15
WD: substitutional Centre I	O1	7.6250	152.74	36.83
(0.8240, 0.7450, 0.9988)	O2	11.2440	180.00	55.38
	O3	6.2035	164.92	52.63
	O4	7.5444	180.00	4.55
	O1’	6.0650	116.35	40.63
	O2’	7.8415	97.19	17.04

ND = No distortion, WD = With distortion

$$\mathcal{H}_{ZFS} = B_2^0 O_2^0 + B_2^2 O_2^2 = \frac{1}{3} b_2^0 O_2^0 + \frac{1}{3} b_2^2 O_2^2 = D(S_z^2 - \frac{1}{3} S(S+1)) + E(S_x^2 - S_y^2) , \quad (2)$$

The traditional orthorhombic ZFS parameters D, E and B_k^q, b_k^q are related as:

$$b_2^0 = D = 3 B_2^0 , \; b_2^2 = 3E = 3 B_2^2 . \quad (3)$$

The parameters of ZFS (in ESO notation) for any symmetry using SPM [20-21] are found as:

$$b_k^q = \sum_i \bar{b}_k (R_0) \left(\frac{R_0}{R_i} \right)^{t_k} K_k^q (\theta_i, \varphi_i) , \quad (4)$$

where (R_i, θ_I, φ_i) are the spherical polar coordinates of i-th ligand. The intrinsic parameters $\bar{b}_k$ provide the strength of the k-th rank ZFS contribution from a ligand at the distance R_i and the coordination factors K_k^q give the geometrical information. K_k^q for k = 1 to 6 in ESO notation [22] are given in Appendix A1 of [23].

Eq. (4) yields traditional ZFS parameters, D and E, in terms of the intrinsic parameters $\bar{b}_k$, the power-law exponents t_k and the reference distance R_0, as [23, 24-26]:

$$b_2^0 = D = \frac{\bar{b}_2(R_0)}{2}\left[\left(\frac{R_0}{R_i}\right)^{t_2}\sum_i (3\cos^2\theta_i - 1)\right]$$

$$b_2^2 = 3E = \frac{b_2^2}{3} = \frac{\bar{b}_2(R_0)}{2}\left[\left(\frac{R_0}{R_i}\right)^{t_2}\sum_i \sin^2\theta_i \cos 2\varphi_i\right] \quad (5)$$

Cr^{3+} ion in $Li_2SO_4.H_2O$ may be assumed to substitute at the Li^+ ion site, and the interstitial site with similar ligand arrangement. The Cr^{3+} ion's local symmetry is supposed to be approximately orthorhombic. In $LiNbO_3$ with octahedral coordination of Cr^{3+} ion having Cr^{3+}-O^{2-} bond, $\bar{b}_2(R_0)$ = 2.34 cm^{-1} and t_2 = -0.12 [27] were used to obtain b_2^0 and b_2^2. Since Cr^{3+} ion in $Li_2SO_4.H_2O$ has distorted octahedral coordination (Fig.1) with oxygen as ligands, the b_K^q in the current research are established using $\bar{b}_2(R_0)$ = 2.34 cm^{-1} and t_2 = -0.77 for center I.

The ligands' spherical polar coordinates and the position of the Cr^{3+} ion displayed in Table 1are considered for calculation. The traditional ZFS parameters, D and E of Cr^{3+} ion in $Li_2SO_4.H_2O$ single crystal are decided using Eq. (5). To determine the ZFS parameters, the reference distance R_0 = 0.200 nm was used [28], and the values are: |D| = 1605.3×10^{-4} $cm^{-1}$and |E| = 33.4 ×10^{-4} cm^{-1} for center I. For symmetry that is orthorhombic, the ratio b_2^2 / b_2^0 should fall between 0 and 1 [29]. In the current calculation, the ratio $|b_2^2| / |b_2^0|$ = 0.062 and |E| / |D| = 0.020 for center I. It is seen that the calculated values of |D| and |E| do not agree with the experimental ones though $|b_2^2| / |b_2^0|$ is in the specified range [29]. Therefore, with above t_2 and reference distance R_0, the ZFS parameters |D| and |E| are calculated for Cr^{3+} at the Li^+ site with distortion having position Li^+(0.8240, 0.7450, 0.9988)for center I. The local environment about Cr3+ is shown in Fig. 2. The traditional ZFS parameters obtained now are |*D*| = 1420.3×10^{-4} cm^{-1}, |*E*| = 177.6×10^{-4} $cm^{-1}$for center I, which correspond well with the values obtained from the experiment. The ratio $|b_2^2| / |b_2^0|$ = 0.375 and |*E*| / |*D*| = 0.125 for center I are in the given range [30]. Further, with above t_2 and reference distance R_0, the ZFS parameters |*D*| and |*E*| are determined for Cr^{3+} at the interstitial site but the values acquired are quite distinct from the values found in the experiment. Therefore, these are not shown here.

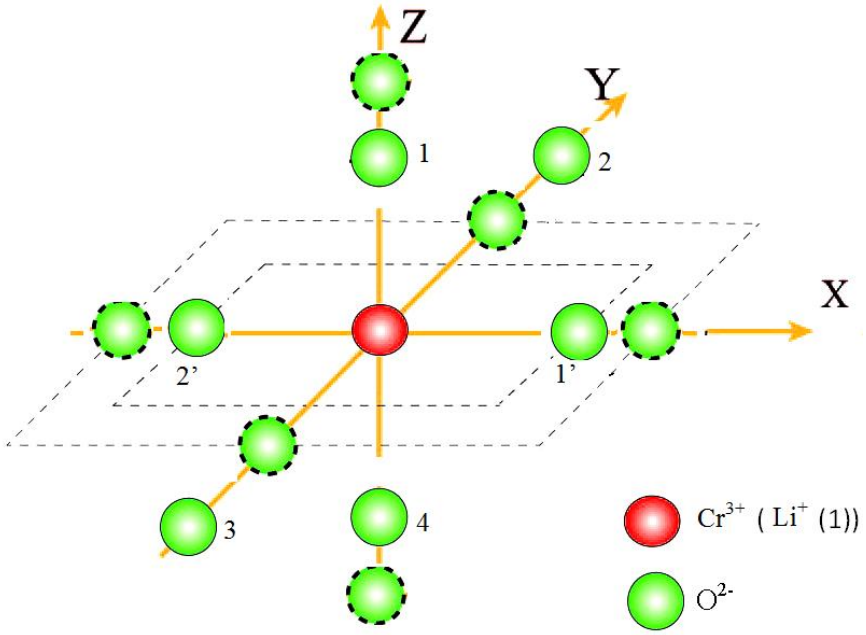

Figure 2. Graphical presentation of local environment (dotted circles show positions after distortion)

Table 2 lists the experimental and calculated ZFS parameters for the Cr^{3+} ion in $Li_2SO_4.H_2O$. This table shows that the ZFS parameters |D| and |E| are in good match with the values of the experiment [11] when the distortion is included into calculation.

Table 2. Calculated and experimental ZFS parameters of Cr^{3+} in $Li_2SO_4.H_2O$ single crystal for center I along with reference distance

		Calculated ZFS parameters (cm^{-1})			Traditional ZFS parameters ($\times 10^{-4} cm^{-1}$)		
Site	R_0 Å	$\lvert b_2^0 \rvert$	$\lvert b_2^2 \rvert$	$\lvert b_2^2 \rvert / \lvert b_2^0 \rvert$	$\lvert D \rvert$	$\lvert E \rvert$	$\lvert E \rvert / \lvert D \rvert$
ND	2.00	0.16053	0.01005	0.062	1605.3	33.4	0.020
Center I							
WD	2.00	0.14203	0.05330	0.375	1420.3	177.6	0.125
					1420.3[e]	177.5[e]	0.124

ND = No distortion, WD = With distortion, [e] = experimental

4. Calculations of crystal field parameters

In crystals [30–33], the CF energy states of transition ions by using Wybourne operators are given by [15, 34, 35]:

$$\mathscr{H}_{CF} = \sum_{kq} B_{kq} C_q^{(k)} \tag{6}$$

where $\mathscr{H}_{CF}$ is CF Hamiltonian. The CF parameters in (6) for a metal-ligand complex are evaluated using SPM [20-21] as follows:

$$B_{kq} = \sum_i \bar{A}_k \left(\frac{R_0}{R_i} \right)^{t_k} K_{kq}(\theta_i, \varphi_i). \tag{7}$$

R_0 is the reference distance, R_i, θ_i, φ_i are the i^{th} ligand spherical polar coordinates and K_{kq} are the coordination factors [30]. $\bar{A}_2$ = 40, 400 cm^{-1}, t_2 = 1.3, $\bar{A}_4$ =11, 700 cm^{-1} and t_4 = 3.4 are used to find B_{kq} (k = 2, 4; q = 0, 2, 4) [30]. Table 3 displays the B_{kq} parameters that were computed. The ratio $|B_{22}|/|B_{20}|$ = 0.184 for center I indicating that B_{kq} parameters are standardized [29]. Using B_{kq} parameters in Table 3 and CFA computer program [31, 32], the CF energy levels of Cr^{3+} ion in $Li_2SO_4.H_2O$ single crystals are calculated by diagonalizing the entire Hamiltonian. Table 4 gives the energy values that were computed. The comparison of calculated energy values is done with the experimental energy values for Cr^{3+}: NiMTH [36] having similar ligands as in $Li_2SO_4.H_2O$since no optical analysis of Cr^{3+} in $Li_2SO_4.H_2O$ single crystal is reported in literature. From Table 4, the experimental and theoretical band positions are seen to be reasonably consistent. Therefore the theoretical study of Cr^{3+} ions at Li^+ sites in $Li_2SO_4.H_2O$supports the experimental one [11, 36].

Table 3. B_{kq} parameters of Cr^{3+} in $Li_2SO_4.H_2O$ single crystal for center I with distortion

		Calculated B_{kq} (cm^{-1}) Parameters used for CFA package					
Site	R_0 Å	B_{20}	B_{22}	B_{40}	B_{42}	B_{44}	$\lvert B22 \rvert / \lvert B20 \rvert$
Center I							
WD	2.00	22741.12	4192.224	2626.792	-428.516	-428.989	0.184

WD = With distortion

The spectra of optical absorption of Cr^{3+}-activated phosphors have been explained using Franck-Condon analysis with the configurational-coordinate (CC) model [37]. The different excited state-ground state transitions in Cr^{3+} are due to strong coupling with the lattice vibrations (CC model) [37]. The CC model is not being used and hence there is difference between excited-state peak energies obtained here and zero-phonon line (ZPL) energies discussed in [37,38].The oxide- phosphors doped with Cr^{3+} are classified into two groups: (i) type O–Cr–A, (ii) type O–Cr–B. The crystal-field strength of type O–Cr–A phosphors fall in the region of Dq/B > 2.1 and, hence, their luminescence properties is determined by the ^2E_g-related luminescence transitions while the crystal-field strength of type O–Cr–B phosphors fall in the region of Dq/B < 2.1 and, so, their luminescence properties is determined by the $^4T_{2g}$-related optical transitions.

$Li_2SO_4.H_2O$: Cr^{3+} comes under O–Cr-A type phosphors (Dq/B =2.649 which is >2.1) [38].

5. Summary and conclusions

The zero-field splitting (ZFS) and crystal field (CF) parametersforCr^{3+} ions in $Li_2SO_4.H_2O$ single crystals are computed employing the superposition model(SPM). Cr^{3+} ions in $Li_2SO_4.H_2O$ crystal at Li^+ ion sites, interstitial site and distortion models are taken up for calculation. The calculated traditional ZFS parameters for Cr^{3+} ion at Li^+ sites in $Li_2SO_4.H_2O$ single crystal give excellent conform to the experimental values when distortion is introduced in the calculation. It is discovered that theCr^{3+} ions substitute at Li^+ ion sites in $Li_2SO_4.H_2O$ lattice with charge compensation. The CF energy values for Cr^{3+} ions at Li^+ sites calculated using CFA package and CF parameters are reasonably in agreement with the experimental ones. Thus, the theoretical findings corroborate the experimental investigation.

Table 4. Energy bands determined through experimentation and computation(center I) of Cr^{3+} in $Li_2SO_4.H_2O$ single crystal

Transition from $^4A_{2g}(F)$	Experimentally observed band (cm^{-1})	Calculated energy band from CFA (cm^{-1})
		Center I
$^2E_g(G)$		13967, 14135
$^2T_{1g}(G)$		15143, 15192, 15630
$^4T_{2g}(F)$	17725	16053, 16334, 16943, 17176, 17218, 17944
$^4T_1g(F)$	24505	22646, 22965, 23427, 24339, 24919, 26075
$^4T_{1g}(P)$		31161, 31466, 34333, 34843, 35405, 37345
$^2T_{1g}(aD)$		39481, 44015, 45117
$^2E_g(bD)$		52393, 54981

(Racah parameters *A*, *B* and *C*, spin-orbit coupling constant and Trees correction are 0, 668, 2672 (= 4B), 276 and 70 cm^{-1}, respectively)

The modeling approach taken up in this work could prove helpful in the future in correlating EPR and optical data for different ion-host systems to investigate crystals for a variety of industrial and scientific applications.

Acknowledgments

The department head of physics is appreciated by the writers for providing the departmental facilities and Prof. C. Rudowicz, Faculty of Chemistry, A. Mickiewicz. University, Poznan, Poland for sending CFA computer program.

References

[1] Umar, M.; Singh, R.; Chand, P.; Upreti, G. Electron paramagnetic resonance study of vanadyl ion doped in α-calcium formate single crystal. *J. Magn. Reson. (1969)* **1985**, *64*, 426–435, https://doi.org/10.1016/0022-2364(85)90105-2.
[2] Mabbs, F.E.; Collison, D.; Gatteschi, D. Electron paramagnetic resonance of d transition metal compounds, Elsevier, Amsterdam, 1992. xx + 1326 pages. $622.00, Dfl. 995.00 ISBN 0-444-89852-2. *Magn. Reson. Chem.* **1994**, *32*, 67–67, https://doi.org/10.1002/mrc.1260320114.
[3] Weil J A, Bolton J R. Electron Paramagnetic Resonance: Elementary Theory and Practical Applications, 2nd ed., New York: Wiley; 2007.
[4] Pilbrow J R. in: Transition Ion Electron Paramagnetic Resonance, Oxford: Clarendon Press; 1990.
[5] Brik, M.; Avram, C.; Avram, N. Calculations of spin Hamiltonian parameters and analysis of trigonal distortions in LiSr(Al,Ga)F6:Cr3+ crystals. *Phys. B: Condens. Matter* **2006**, *384*, 78–81, https://doi.org/10.1016/j.physb.2006.05.155.
[6] Pandey S, Kripal R, Yadav A K, Açıkg¨oz M, Gnutek P, Rudowicz C. Implications of direct conversions of crystal field parameters into zero-field splitting ones - Case study: Superposition model analysis for Cr3+ ions at orthorhombic sites in LiKSO4. J. Lumin. 2021; 230: 117548 (10 pages).
[7] Bradbury, M.; Tewman, D. Ratios of crystal field parameters in rare earth salts. *Chem. Phys. Lett.* **1967**, *1*, 44–45, https://doi.org/10.1016/0009-2614(67)80063-0.
[8] Salotkar, K.S.; Patle, S.K.; Maske, V.D.; Khan, A.Z.; Bhonsule, S.U.; Rewatkar, K.G.; Ugemuge, N.S. Influence of dopant on characteristics of lithium sulfate monohydrate single crystal. PROCEEDINGS OF THE INTERNATIONAL CONFERENCE ON MATHEMATICAL SCIENCES AND

TECHNOLOGY 2022 (MATHTECH 2022): Navigating the Everchanging Norm with Mathematics and Technology. LOCATION OF CONFERENCE, MalaysiaDATE OF CONFERENCE; .
[9] Naik, M.M.; Mir, F.A.; Ullah, F.; Ahmad, P.A.; Ghayas, B. A brief study on structural, optical, and photovoltaic properties of lithium sulfate monohydrate single crystals. *J. Mater. Sci. Mater. Electron.* **2020**, *31*, 11855–11861, https://doi.org/10.1007/s10854-020-03739-3.
[10] Bansal, R.; Seth, V.; Chand, P.; Gupta, S. EPR and optical spectra of vanadyl ion (impurities) in three polycrystalline solids. *J. Phys. Chem. Solids* **1991**, *52*, 389–392, https://doi.org/10.1016/0022-3697(91)90088-h.
[11] Çelik, F.; Köksal, F.; Kartal, I.; Gümüş, H. EPR Study of VO2+ and Cr3+ in Li2SO4 · H2O Single Crystal. **1997**, *52*, 765–770, https://doi.org/10.1515/zna-1997-1102.
[12] Hirahara, E.; Murakami, M. Nuclear Magnetic Resonance Experiment on the Single Crystal Of Lithium Sulfate Monohydrate, $Li_2SO_4H_2O$. *J. Phys. Soc. Jpn.* **1956**, *11*, 239–244, https://doi.org/10.1143/jpsj.11.239.
[13] MacGrath J W, Silvldi A A, Carroll J C. Proton Magnetic Resonance Study of Lithium Sulfate Monohydrate. J. Chem. Phys. 1959; 31:1444-1449.
[14] Larson A C. The Crystal Structure of Li2SO4.H2O. A Three-Dimensional Refinement. Acta Cryst. 1965; 18: 717-724.
[15] Rudowicz, C.; Karbowiak, M. Disentangling intricate web of interrelated notions at the interface between the physical (crystal field) Hamiltonians and the effective (spin) Hamiltonians. *Co-ord. Chem. Rev.* **2015**, *287*, 28–63, https://doi.org/10.1016/j.ccr.2014.12.006.
[16] Rudowicz C. Concept of spin Hamiltonian, forms of zero field splitting and electronic Zeeman Hamiltonians and relations between parameters used in EPR. A critical review. Magn. Reson. Rev. 1987; 13: 1-89; Erratum, Rudowicz C. Magn. Reson. Rev. 1988; 13: 335.
[17] Rudowicz, C.; Misra, S.K. SPIN-HAMILTONIAN FORMALISMS IN ELECTRON MAGNETIC RESONANCE (EMR) AND RELATED SPECTROSCOPIES. *Appl. Spectrosc. Rev.* **2001**, *36*, 11–63, https://doi.org/10.1081/asr-100103089.
[18] Rudowicz, C. Transformation relations for the conventional Okq and normalised O'kq Stevens operator equivalents with k = 1 to 6 and -k $\leq$ q $\leq$ k. *J. Phys. C: Solid State Phys.* **1985**, *18*, 3837–3837, https://doi.org/10.1088/0022-3719/18/19/522.
[19] Rudowicz, C.; Chung, C.Y. The generalization of the extended Stevens operators to higher ranks and spins, and a systematic review of the tables of the tensor operators and their matrix elements. *J. Physics: Condens. Matter* **2004**, *16*, 5825–5847, https://doi.org/10.1088/0953-8984/16/32/018.
[20] Newman D J, Ng B. Superposition model. Ch. 5 in: Newman D J, Ng B. (Eds.). Crystal Field Handbook. UK: Cambridge University Press; pp. 83–119, 2000.
[21] Newman D J, Ng B. The Superposition model of crystal fields. Rep. Prog. Phys. 1989;52: 699-763.
[22] Rudowicz, C. On the derivation of the superposition-model formulae using the transformation relations for the Stevens operators. *J. Phys. C: Solid State Phys.* **1987**, *20*, 6033–6037, https://doi.org/10.1088/0022-3719/20/35/018.
[23] Rudowicz, C.; Gnutek, P.; Acikgoz, M. Superposition model in electron magnetic resonance spectroscopy - a primer for experimentalists with illustrative applications and literature database. *Appl. Spectrosc. Rev.* **2019**, *54*, 673–718, https://doi.org/10.1080/05704928.2018.1494601.
[24] Açıkgöz, M. A study of the impurity structure for 3d3 (Cr3+ and Mn4+) ions doped into rutile TiO2 crystal. *Spectrochim. Acta Part A: Mol. Biomol. Spectrosc.* **2012**, *86*, 417–422, https://doi.org/10.1016/j.saa.2011.10.061.
[25] Müller KA, Berlinger W, Albers J. Paramagnetic resonance and local position of Cr3+ in ferroelectric BaTiO3. Phys. Rev. B 1985; 32(9): 5837-5850.
[26] Müller K A, Berlinger W. Superposition model for sixfold-coordinated Cr3+ in oxide crystals (EPR study). J. Phys. C: Solid State Phys. 1983; 16(35): 6861-6874.
[27] Yeom, T.; Chang, Y.; Rudowicz, C.; Choh, S. Cr3+ centres in LiNbO3: Experimental and theoretical investigation of spin hamiltonian parameters. *Solid State Commun.* **1993**, *87*, 245–249, https://doi.org/10.1016/0038-1098(93)90485-6.
[28] Siegel, E.; Müller, K.A. Structure of transition-metal—oxygen-vacancy pair centers. *Phys. Rev. B* **1979**, *19*, 109–120, https://doi.org/10.1103/physrevb.19.109.
[29] Rudowicz, C.; Bramley, R. On standardization of the spin Hamiltonian and the ligand field Hamiltonian for orthorhombic symmetry. *J. Chem. Phys.* **1985**, *83*, 5192–5197, https://doi.org/10.1063/1.449731.
[30] Yeung YY, Newman D J. Superposition-model analyses for the Cr3+ 4A2 ground state. Phys. Rev. B 1986; 34(4): 2258-2265.
[31] Yeung, Y.; Rudowicz, C. Ligand field analysis of the 3dN ions at orthorhombic or higher symmetry sites. *Comput. Chem.* **1992**, *16*, 207–216, https://doi.org/10.1016/0097-8485(92)80004-j.

[32] Yeung, Y.; Rudowicz, C. Crystal Field Energy Levels and State Vectors for the 3dN Ions at Orthorhombic or Higher Symmetry Sites. *J. Comput. Phys.* **1993**, *109*, 150–152, https://doi.org/10.1006/jcph.1993.1206.
[33] Chang Y M, Rudowicz C, Yeung YY. Crystal field analysis of the 3dN ions at low symmetry sites including the 'imaginary' terms. Computers in Physics 1994; 8(5): 583-588.
[34] Wybourne, B.G.; Meggers, W.F. *Spectroscopic Properties of Rare Earths*. *Phys. Today* **1965**, *18*, 70–72, https://doi.org/10.1063/1.3047727.
[35] Figgis B N, Hitchman M A. Ligand Field Theory and its Applications. New York: Wiley; 2000.
[36] Gopal NO, Narsimhulu KV, Sunandan C S, Rao J L. EPR and optical absorption spectral studies of Cr3+ ions doped in nickel maleate tetrahydrate single crystals. Physica B 2004; 348(1-4): 335-340.
[37] Adachi, S. Photoluminescence Spectroscopy and Crystal-Field Parameters of Cr^{3+} Ion in Red and Deep Red-Emitting Phosphors. *ECS J. Solid State Sci. Technol.* **2019**, *8*, R164–R168, https://doi.org/10.1149/2.0061912jss.
[38] Adachi S. Review—Photoluminescence Properties of Cr3+-Activated Oxide Phosphors. ECS J Solid State Sci. Tech. 2021; 10: 026001(21 pages).